RESEARCH ARTICLE

Kinetic Microscale Thermophoresis

Julian A. C. Stein[a], Alan Ianeselli[a] and Dieter Braun*[a]

[a] Julian Stein, Alan Ianeselli, Prof. Dr. Dieter Braun
Systems Biophysics, Department of Physics
Ludwig-Maximilians-Universität München and Center for NanoScience
Amalienstaße 54, 80799 München (Germany)
E-mail: dieter.braun@lmu.de

Supporting information for this article is given via a link at the end of the document.

Abstract: We established an extension of Microscale Thermophoresis (MST) to measure binding kinetics together with binding affinity in a single experimental run, by increasing the thermal dissipation of the sample. After the switch-off of an IR laser, that locally heated the sample, the temperature re-equilibrated within 250 ms. The kinetic relaxation fingerprints were extracted from the fluorescence changes back to thermodynamic equilibrium. We measured DNA hybridization on-rates and off-rates in the range between 10^4-10^6 $M^{-1}s^{-1}$ and 10^{-4}-10^{-1} s^{-1}, respectively. We observed the expected exponential dependence of the DNA hybridization off-rates on salt concentration, strand length and inverse temperature. The measured on-rates showed a linear dependence on salt and a weak if no dependence at all on length and temperature. For biological binding reactions with sufficient enthalpic contributions, Kinetic MST offers a robust and immobilization-free determination of kinetic rates and binding affinity and also in crowded solutions.

Introduction

Binding processes of biological molecules play a fundamental role in almost all facets of living matter. The dissociation constant $K_d = k_{off}/k_{on}$ characterizes the affinity of a binder-ligand system and has been extensively studied in many research fields.[1–4] K_d are usually determined by the analysis of equilibrated states of binder-ligand systems.[5] The measurement of the underlying kinetic association and dissociation rates k_{on} (on-rate) and k_{off} (off-rate) requires the transition from a non-equilibrium state towards equilibrium. The knowledge of the kinetic rates provides a more thorough understanding of binding processes, as they characterize the forming (on-rate dependent) stability and unbinding (off-rate dependent) of the bound complex. Biomolecular on-rates range from 10^3 to 10^9 $M^{-1}s^{-1}$ and off-rates from 10^{-5} to 1 s^{-1}.[6] The knowledge of the on-rate and off-rate of a binder-ligand complex thus can improve the dosation and frequency of drug intake. However, the quantification of kinetic rates has not received as much attention as the binding constant.[7,8]

Kinetic rates of binder-ligand systems are experimentally accessible by measuring the time-resolved transition from the unbound state towards the fully bound state.[5] During this transition, the change in concentration of bound and unbound complexes, is governed by the kinetic rates.[8] Consequently, an experimental setup to measure kinetic rates not only needs to be capable of detection of binding but also needs to allow for time-resolved measurement of transition between the states. Thereby the deflection from equilibrium can be done by rapid mixing of the reactants, or rapid temperature jumps. Both approaches have advantages and disadvantages which are decisive for the respective applications.

To provide fast mixing, many methods of measuring the kinetic rates by rapidly mixing the reactants rely on the immobilization of one of the reactants. The immobilized binder is then exposed to the ligand for a defined period and the subsequent binding is recorded, e.g. by surface-plasmon resonance measurements (SPR),[9] nanotube-biosensors biolayer interferometry (BLI)[10] and stopped flow fluorescence spectroscopy.[5,11] SPR and BLI benefit from label-free detection, real-time data acquisition as well as their independence on temperature-related characteristics, i.e. a temperature to deflect the system out of equilibrium. Immobilization-based methods that apply electric potentials to expose the ligand and the binder are e.g. aptamer-analyte interactions.[12] However, due to immobilization, the chemical and physical properties of the reactant can undergo changes, possibly changing the conformation and stability of the reactants.[13] Further, the binding event could be inhibited,[14] e.g. the binding site could be inaccessible due to random orientation of the attached molecule to surface.[15] Also the strength of the binding could be overestimated due to underestimated slow off rates, an effect reported for in SPR.[1,16] The use of immobilization techniques offers suitable characterization for interactions near or on surfaces.

However, physiological interactions take place in free or crowded solutions. Experimental methods which access kinetic rates under such conditions – without immobilizing one of the reactants – are fluorescence anisotropy (FA),[17] fluorescence correlation spectroscopy (FCS), Förster Resonance Transfer (FRET)[18] and fluorescence quenching (coupled to stopped-flow technique)[19] among others.[20] Drawbacks of these methods are the requirement of comparatively large changes in conformation upon binding and the labeling of at least one of the reactants with a fluorescent dye. The attached fluorescent label also possibly changes the behavior of the binding properties of the molecule.[21]

This work presents a novel method called Kinetic Microscale Thermophoresis (KMST) to access kinetic reaction rates immobilization-free, purely optical and in bulk. KMST is a natural extension to the established and often used method of Microscale Thermophoresis (MST).[22–27] MST utilizes the binding-dependent intensity change of fluorescently-labeled molecules in microscopic temperature gradients to measure binding affinities and can further detect minute changes in conformation, charge, size of molecule, as they are induced by a binding event, enzymatic activities and modifications of proteins and nucleic acids.[21] By increasing the thermal dissipation of the sample-

containing capillary (Fig.1) an MST setup incorporates the technique of temperature jumps. Appropriate treatment of the temperature-related, bleaching, diffusion, thermophoretic and kinetic contribution to the fluorescence signal (Fig.1 a & Fig.2) allows for determination of the binding affinity and the kinetic rates in a single experimental run (Fig.3). We show that the relaxation speed $\tau_{kinetic}^{-1}$ can be detected in the range from 0.01 to 0.5 s^{-1}, enabling for measurements of k_{on} between 10^4 and 10^6 $M^{-1}s^{-1}$ and k_{off} between 10^{-4} and 0.1 s^{-1}. To demonstrate the method's effectiveness, we systematically measured the kinetic hybridization rates for fully-complementary DNA strands between 10bp and 16bp under various buffer conditions (Fig.4 & 5): the off-rates showed exponential dependence on strand length, temperature and salt concentrations. The on-rates showed weak dependence on strand length and temperature and linear dependence on salt concentration. Moreover, an analysis of the temperature dependence of the kinetic rates shed light into the hybridization mechanism of DNA and summarized the determinants of DNA binding. Finally, we show that with KMST the hybridization of DNA in crowded solutions can be determined with only minor loss of accuracy.

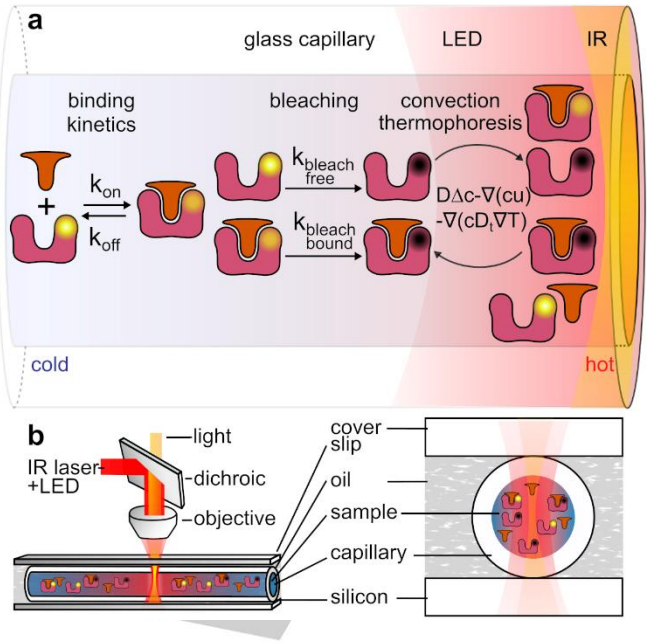

***Figure. 1: Kinetic Microscale Thermophoresis setup. a** Molecular interaction processes that change the detected fluorescence of the sample. **b** To obtain a strong thermal coupling, the sample solution inside a capillary is placed between a temperature-controlled silicon plate and a glass cover slip, surrounded with immersion oil and locally heated with an IR-laser. Through the same objective, fluorescence emission and excitation LED light is detected by a photodiode.*

Results and Discussion

Binding kinetics from Kinetic Microscale Thermophoresis

A KMST setup was obtained by modifying a conventional MST setup (Nanotemper Monolith(R) NT.115^{Pico}) by placing the sample containing capillary on a silicon plate and immersing with oil, see Fig.1 a & b. The fluorescence excitation/detection unit of the NT.115 Pico measured the fluorescence intensity change over time in a localized spot of the sample, see Fig.1 b. Through the same objective as the fluorescence detection unit, an infrared laser with an emission wavelength of 1480 nm was focused to the center of the capillary to create a temperature gradient within the capillary for a defined time period. The strong thermal coupling provided quick formation and reduction of the temperature gradient in less than 250 ms, see SI.Fig.1. Averaged over the volume, the temperature gradient spanned about 10 K and led to convection and thermophoretic movement of the binder and the ligand,[1] see SI-1.

The binding affinity K_d and the kinetic parameters k_{on} and k_{off} were obtained by fluorescence measurements of a dilution series with a constant (labeled) binder B^*_{tot} and increasing ligand concentration L_{tot}. Each measurement could be divided in three successive phases (Fig.2). In the pre heat phase, the bound sample's equilibrium K_d and binding curve were determined by fitting Eq.1(SI) to the measured bleaching rates k_{bleach} of the traces,[24] see Fig.3 a and SI-2. In the successive heat phase, the sample was heated by the IR-laser for 40 seconds, the bound complex unbound and the fluorescence decreased due to the increased temperature.[26] The fluorescence traces were governed by thermophoretic movement, convection, bleaching and kinetics, from which the kinetic fingerprint could not be extracted reliably enough, see SI-3. When the IR-laser was switched off, the system returned to thermal equilibrium within 250 ms. In this so called post heat phase, the kinetic fingerprint could be extracted from the fluorescence signal by appropriate analysis: the bleaching and diffusion contributions were elucidated from the pre heat phase and the zero-ligand trace in the post heat phase, respectively. Then, the fluorescence traces of the post heat phase were corrected for the bleaching and diffusion for each ligand concentration, respectively, and exponential kinetic relaxation was fitted to $F_{kinetic} \propto exp(-t/\tau_{kinetic})$, see Eq.7(SI) in SI-4. The resulting inverse kinetic relaxation constants were plotted against the total ligand concentration (Fig.3 b). The on rate k_{on} was fitted according to Eq.2(SI), see Fig.3c, and k_{off} could be obtained.

To validate the experimental results, we performed finite element simulations with COMSOL Multiphysics which captured the relevant interaction characteristics of heating, laminar flow, bleaching and reaction kinetics of diluted species in the sample capillary, see simulated yellow fluorescence traces in Fig.2 and SI-5. The simulated fluorescence traces were similar to the experimental traces and their analysis yielded for similar kinetic rates, suggesting coherency of experimental observation and analysis with theoretical expectation based on fundamental rate-equations.

KMST profits from the advantages from the widely-used MST technique:[1,21–24,26] significant, reliable and reproducible data acquisition, as well as low cost and consumption of samples. Importantly, a KMST and MST measurement only requires one of the reactants to be labeled (instead of both) which facilitates sample preparation and ultimately minimizes label-related interferences within the binding process. Further, the determination of the kinetic rates together with the binding affinity is performed in a single step within the same biological sample. Taken together, KMST provides a suitable technique with minor technique-related systematic measurement error. A volume of less than 5µl and around nM concentrations for labeled binder and up to µM concentrations for ligand brings down the costs for the measurement of one affinity.[1] The dilution series, the capillary

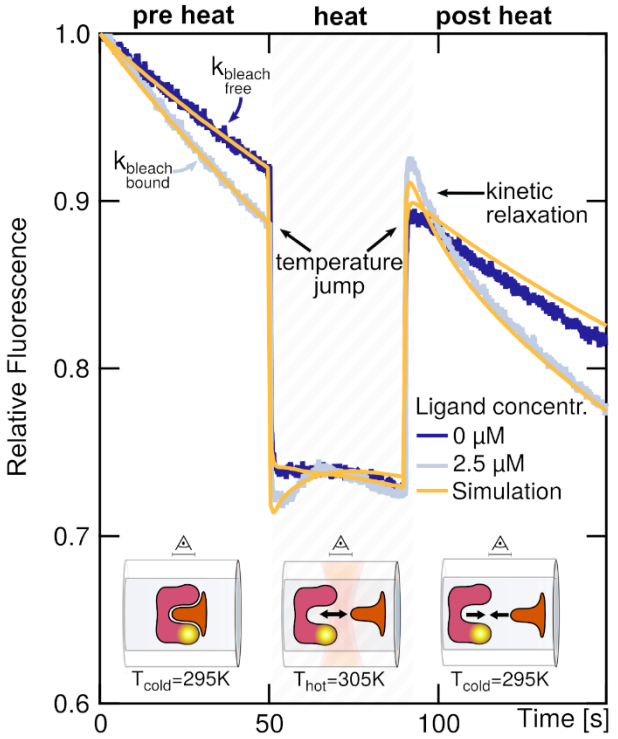

Figure 2: Fluorescence traces unravel kinetics *In the pre heating phase, the fluorophore bleached due to LED illumination. The bleach rate was higher for the bound complex. During the heating phase with IR laser, the fluorescence quickly changed upon the temperature jump within 250 ms. Then, the fluorescence change resulted from unbinding, bleaching, convection and thermophoresis. In the post heating phase, the sample quickly returned to ambient temperature. The fluorescence change was governed by kinetic relaxation from unbound state towards the bound state. Fluorescence traces are shown for 0µM and 2.5µM of 12mer DNA strands (dark and light blue) at 19°C with 2 nM complementary labeled binder strand and COMSOL simulations (yellow), respectively.*

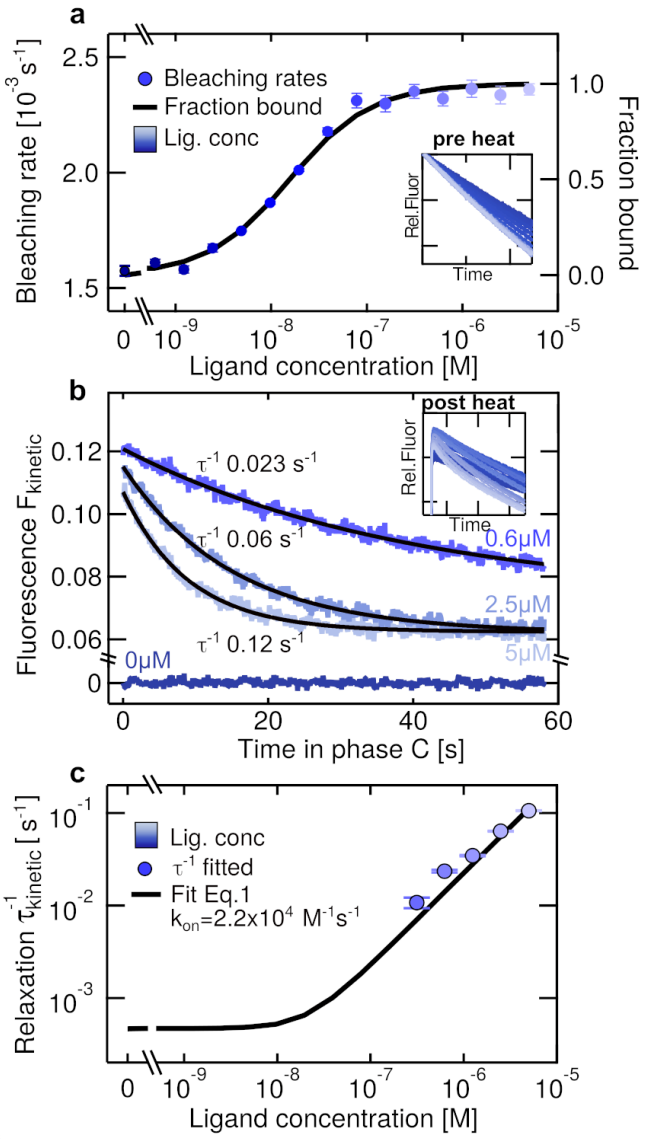

Figure 3: Kinetic data extraction a *The binding curve and K_d obtained by plotting the bleaching rate in the pre heat phase against the ligand concentration.* ***b*** *Kinetic relaxation traces obtained by analyzing the fluorescence traces in the post heat phase. The insets show all measured fluorescence curves of one dilution series.* ***c*** *The fitted $\tau^{-1}_{kinetic}$ were plotted over the ligand concentration to fit the on-rate according to Eq.2(SI), for fully-complementary 12mer in 0.1xPBS at 16°C, we yield k_{on}=2.2x10^4 M^{-1}s^{-1} and k_{off}=2.4x10^{-4} s^{-1}.*

filling, the placement of the capillaries on the silicon plate and immersion with oil do not require high-precision adjustments or handling. Data analysis is not dependent on complex theoretical models and is robust against single capillary uncertainties. Like MST, KMST can be used for high-throughput kinetic rate determination.

To extract a kinetic fingerprint from KMST, the ligand-binder system does not necessarily have to be dependent on a size change upon binding. Eventually, a conformation change upon binding, that leads to different fluorescence levels of the bound and unbound state, is sufficient to detect kinetic rates. Control measurements in which the complementary bases had a distance of 4 base pairs to the fluorescent label yielded for similar affinities and kinetic rates, see SI-6. We conclude that a change of the electronic configuration of the Cy5-fluorophore due to distant binding is sufficient to detect binding and thus kinetics. We also performed simulations to test, if kinetics can be extracted reasonably from systems with large size differences of the binder and the ligand, see SI-7. The results suggest that the analysis is robust against large size differences of the reactants (i.e. tenfold increased diffusion coefficient of ligand or binder), and if possible the larger reactant should be labeled to reduce systematic errors within the kinetic rate analysis.

We discuss four conditions which contribute to optimal experimental rate determination, see SI-8 for details. First, reliable fluorescence detection due to sufficient fluorescence signal was optimal for B_{tot}>1nM which allows for robust analysis of binding affinities K_d>1nM. Second, $\tau^{-1}_{kinetic} \ll \tau^{-1}_{cooling}$ is necessary to correctly apply the rate analysis equations and clearly dissect the kinetic contribution from the temperature jump within the fluorescence signal. Third, as the measurements depend temperature-dependent (un)binding, the studied system requires a significant enthalpic contribution ΔH^0. Fourth, the quantum yield of the fluorescence label is required to exhibit a dependence on binding in order to yield for kinetic fingerprint in the fluorescence traces.

The range of measurable on-rates and off rates was comparable with label-free methods, such as SPR,[30] which is capable to measure in a range of 10^3 M^{-1}s^{-1}< k_{on} <10^8 M^{-1}s^{-1} and 10^{-6} s^{-1}< k_{off} <1 s^{-1}.[31] Yet, the limitations for measuring high on-rates with KMST and SPR differ: Whereas SPR is limited by mass transportation and requires molecules of great molecular mass, KMST is limited by the speed of the temperature jump and small

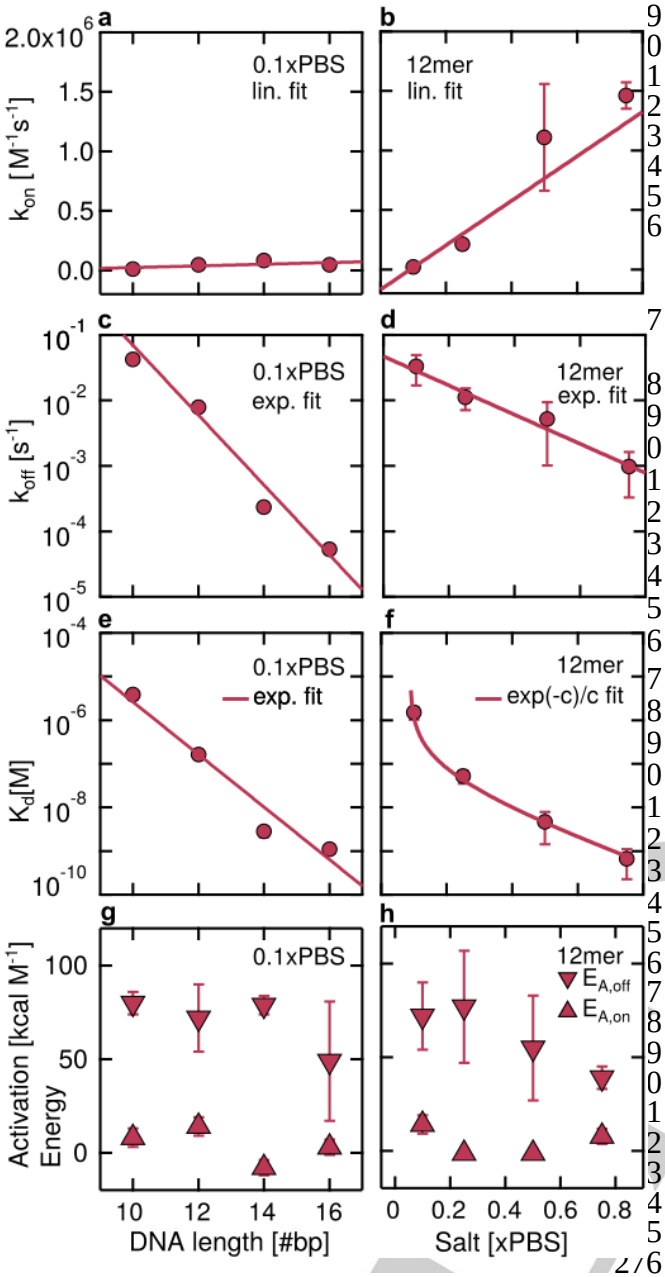

Figure 4: Strand length and salt dependence of k_{on}, k_{off}, K_d and E_A a *The on-rate did not show strand length dependence but* ***b*** *linear salt dependence. The off-rate decreased exponentially with* ***c*** *strand length and* ***d*** *salt concentration.* ***e*** *The resulting equilibrium constant $K_d=k_{off}/k_{on}$ decreased exponentially with length and* ***f*** *according to $K_d \propto e^{-c_{PBS}}/c_{PBS}$ with PBS concentration.* ***g & h*** *Arrhenius activation energy E_A for on-rate and off-rate. Length (salt) dependence was measured at 22°C (25°C).*

K_d<1nM in combination with fast kinetics.[32] KMST profits from its applicability to measure a range of salt concentration and in the crowded solutions with minor loss of accuracy (see below). In contrast to surface-related kinetic measurement methods where sensor response and nonspecific electrostatic binding both increase for decreasing ionic strength.

The comparison of the obtained results by KMST with literature suggest two conclusions: First, the absolute values of the kinetic rates reported by the various methods showed significant differences up to several orders of magnitude for the kinetic rates. This suggests that the kinetic rates strongly depend on the observed system's parameters, e.g. buffer, immobilization, fluorescent labels, temperature and other boundary conditions. KMST shows to be a technique to measure kinetic rates over a broad range – on/off-rates by two/three orders of magnitude – that accomplishes a reduction of these interfering parameters, by reducing the amount of labeled strands to one. Second, the exponential dependence of the off-rates on strand length, temperature and salt concentrations could be shown by the various methods, respectively. For the on-rates, temperature and length dependence remain debated.

DNA hybridization kinetics

The hybridization kinetics of complementary DNA strands of different lengths were measured under various buffer and temperature conditions, see SI-9. All rates measured with KMST are summarized in SI-10. Kinetics measurements with a temperature-jump technique[33] and added Eva Green intercalating dye did not yield for kinetic fingerprints, see SI-10. The measured on-rates showed weak if no dependence on strand length and increased linearly with salt concentration $(1.9 \pm 0.2) \times \frac{10^6 M^{-1} s^{-1}}{xPBS}$, see Fig.4 a & b. The measured off-rates showed exponential dependence on strand length (characteristic length 0.81[bp]) and salt concentration (characteristic concentration 0.19[xPBS]) as seen in Fig.4 c & d. The dissociation constant K_d was strongly dominated by the respective off-rate dependence on strand length (characteristic length 0.72[bp]) and on salt concentration, see Fig.4 e & f. It showed an exponential dependence on strand length and $K_d \propto e^{-c_{PBS}}/c_{PBS}$ dependence on PBS concentration.

The comparison of the absolute values of the measured rates with literature is difficult due to the many different measurement methods and sequences used. We discuss the measured values with regard to the order of magnitude measured, their dependence on the salt concentration, strand length and temperature.

For high salt concentrations (1xPBS), Surface Plasmon Fluorescence measurements report 10^4 $M^{-1}s^{-1}$ [34] which is an order of magnitude smaller than our measurement. FRET measurements for 9mers reported on-rates in the low 10^6 $M^{-1}s^{-1}$ range[35] (with 50mM HEPES), similar to our findings. Measurements with TOOL reported on-rates in the order of 10^6-10^7 $M^{-1}s^{-1}$ [36] for 12mer and 16mer complementary DNA strands, which is an order of magnitude larger than our findings. For low salt concentrations (<0.1xPBS) FRET measurements found on-rates of 10mers to be about 10^4 $M^{-1}s^{-1}$ [18] in free solution buffer, also found in works with Quartz Crystal Microbalance[37] of immobilized 10mers, similar to our results. Multi-channel graphene bionsensors report 10^5 $M^{-1}s^{-1}$ [7] for immobilized target strands, which is an order of magnitude higher than our findings. Our works suggest on-rates for low salt concentrations to be in the range of 10^4-10^5 $M^{-1}s^{-1}$ linearly increasing with salt concentration up to 10^6 $M^{-1}s^{-1}$ for 0.75xPBS, see Fig.4 b, similarly reported earlier.[38]

We observed on-rates to be independent of the strand length, see Fig.4 a, similarly reported earlier.[39] But literature also reported contrarily dependence.[18,36,37] Bielec et al argue that the higher total charge of the longer strands pose a higher energetic barrier for hybridization, especially for low ionic salt environments.[18] Our finding is limited to a strand length difference of 6 by a total length of 16, which may be too short to

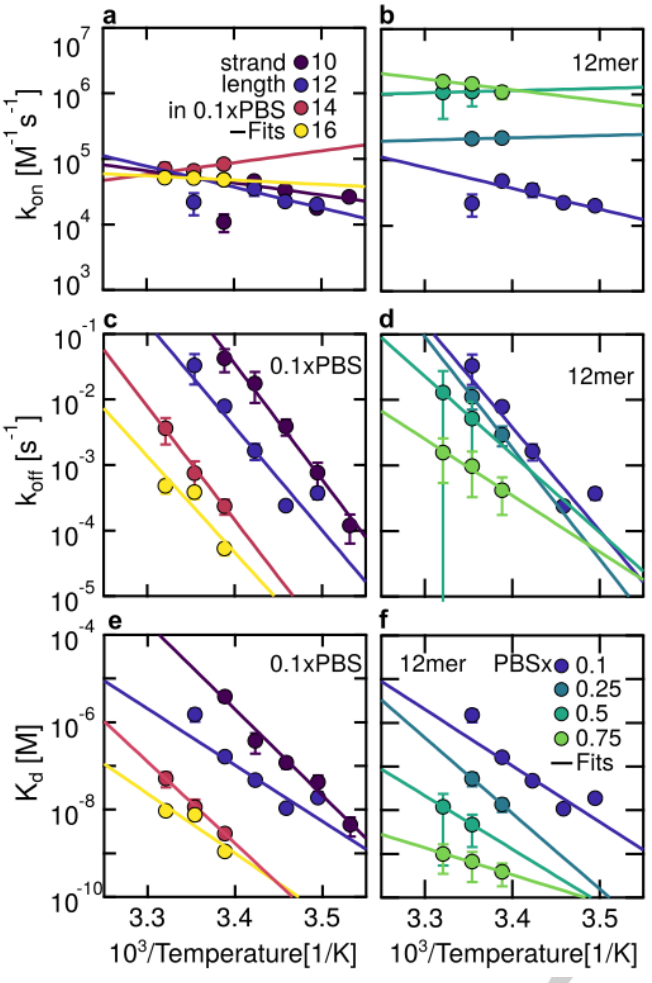

Figure 5: Temperature dependence of K_d, k_{off} and k_{on} of fully-complementary DNA strands a-d *Eyring plots of transition state theory of on-rates and off-rates.* ***a&b*** *On-rates show no strong temperature or strand length dependence.* ***c&d*** *the corresponding off-rates decrease with 1/T* ***e & f*** *Van't Hoff plot for various lengths in 0.1xPBS and salt conditions for 12mer. K_d decreases exponentially with 1/T and decrease for increasing salt concentrations and strand length.*

observe strand-dependent on-rates. The comparison of our rates with the results presented by Okahata et al.[37] is limited due to the immobilization of their used probes.

Literature reported both smaller and larger off-rates for low and high ionic salt conditions than our results suggest, respectively. For low salt concentrations (<0.1xPBS), FRET measurements of Bielec et al.[18] reported off-rates two orders of magnitude smaller than ours. Morrison and Stols[39] found higher off-rates at much higher salt concentrations of 10xPBS in temperature jump experiments. Tawa et al[34] measured smaller off-rates for longer strands in higher salt concentrations. Our measured off-rates showed an exponential decrease with salt concentration, see Fig.4 d, also reported by Okahata et al.[37] and qualitatively supporting Braunlin et al.[38] The exponential decrease of the off-rates with strand length, see Fig.4 c, was in agreement with literature.[32,37,39,40]

DNA hybridization thermodynamics

The measurements of the binding affinity and the kinetic rates for various temperatures allowed for thermodynamic analysis. The Van't Hoff plot was obtained by

$$ln(K_d^0/K_d) = \frac{-\Delta H^0}{RT} + \frac{\Delta S^0}{R}$$

with the standard enthalpy ΔH^0 and standard entropy ΔS^0 which were fitted to K_d values of Fig.5 e & f under K_d^0 =1[M] standard conditions at 295 K, see SI-11. R=1.987 cal K^{-1} mol^{-1} is the gas constant. ΔG^0 and $T\Delta S^0$ were calculated $\Delta G^0 = \Delta H^0 - T\Delta S^0$ accordingly. For increasing temperature, the bound state destabilizes and K_d increases. The negative slope and positive intercept of the Van't Hoff fits yield for $\Delta H^0 < 0$ and $\Delta S^0 < 0$.

The Van't Hoff plots provide support of ΔH^0 to be in the range of about -60 kcal mol^{-1}, and ΔS^0 between -170 and -270 cal K^{-1} mol^{-1}, also reported by surface-tethered FRET measurements[35] and slightly above previously reported values of 8mers measurements with NMR.[38] Additional melting curve measurements of the 12mer strands and associated Van't Hoff analysis yielded for similar K_d dependence on inverse temperature and ΔH^0, see SI-11 and SI-Fig.5 b. At room temperature, both contributions cancel out and yield for rather small negative ΔG^0, supporting the view that DNA hybridization is a spontaneous process:[35,41] the formation of hydrogen bonds and base stacking lead to the exothermic release of heat and the decrease in entropy results from reduced conformational flexibility in the bound state.[42,43] Our findings contribute to the understanding that increased cationic strength increases ΔH^0 and ΔS^0, both becoming less negative. Although ΔH^0 increases with cationic strength $T\Delta S^0$ increases stronger, resulting in a net more negative ΔG^0, thus favoring the bound. However, the meaningfulness of ΔG^0 allows only for limited conclusions, due to large errors, see SI-11. For increasing strand length, we found that ΔH^0 and ΔS^0 increase, resulting in a decrease of ΔG^0, favoring the hybridized state, also reported earlier.[35]

The measured temperature dependence of the on-rates and off-rates allowed for determination of the Arrhenius activation energies $E_{A,on}$ $E_{A,off}$ according to $k = A \cdot exp(-E_A/RT)$ with k the on-rate or off-rate and A the pre-exponential factor, see Fig.4 g & h. The corresponding Arrhenius plots are shown in Fig.5 a - d. All values are summarized in SI-12. Note that E_A are identical to $\Delta H^{\ddagger}$ for the on-rate and off-rate, respectively, due to the applied analysis method.

The on-rates showed no if slight increase with temperature, see Fig.5 a & b, corresponding to smallpositive $E_{A,on} \approx 0$ kcal M^{-1}. $E_{A,on}$ did not show significant dependence on strand length or salt concentration, see in Fig.4 g & h. The temperature dependence of on-rates of DNA hybridization is still object of open debate. Literature reports increasing[39] (for $T<T_{melt}$), decreasing[32] and non-monotonic[37,44] behavior. Our findings contribute insofar, as the determined E_A slightly above and below zero can not be used to exclude one of the proposed hypotheses.

The off-rates showed expected exponential dependence on inverse temperature,[32,37,39,40] see Fig.5 c & d. The measured $E_{A,off}$ became smaller for increasing strand lengths and salt concentrations, see Fig.4 g & h. This is in line with the view that the electrostatic repulsion between the anionic chains of the DNA strands decreases for high ionic salt concentrations and in result stabilize the hybridized bonds.[37] Similar behavior was also found for DNA hairpins.[45]

Identifying the Arrhenius activation energies with the thermodynamic quantities of the Eyring-Polanyi equation (that is $E_{A,on} \equiv \Delta H^{\ddagger}{}_{on}$ and $E_{A,off} \equiv \Delta H^{\ddagger}{}_{off}$) allowed for a connection of kinetic quantities with thermodynamic quantities,[35,41] but in general involves conceptual difficulties.[46] Following this

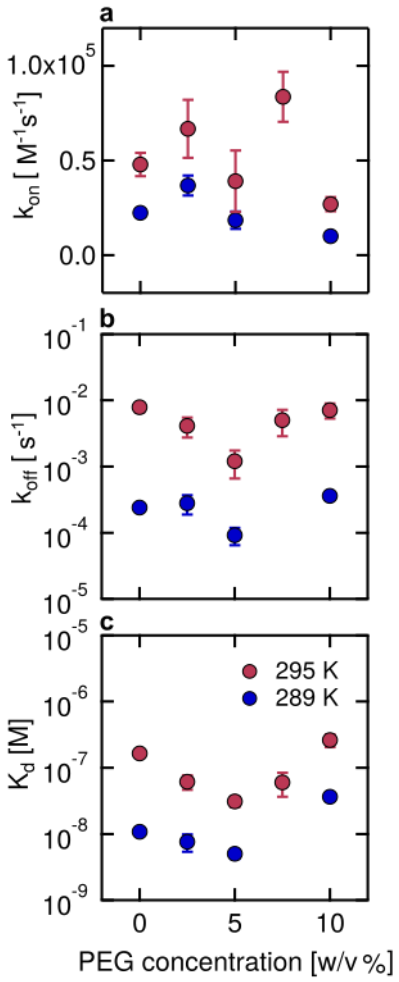

Figure 6: Hybridization rates k_{on}, k_{off} and K_d of fully-complementary 12mer DNA strands in crowded solutions with PEG 8000 a *The on-rates do not show significant dependence on PEG concentrations* ***b*** *Off-rates show decreasing (<5% PEG) and increasing (5-10%PEG) behavior* ***c*** *The resulting K_d are dominated by the off-rate dependence on PEG. All measurements were conducted in 0.1xPBS with 0.05% Tween.*

identification, the thermodynamic enthalpy and entropy landscapes of free state, transition state and bound state could be determined, see SI-12.

DNA hybridization kinetics in crowded solutions

Lastly, we show that KMST allows for measurements of kinetic rates in various fluids with minor loss of accuracy. DNA hybridization takes place in more crowded fluids than pure buffer solutions, but the measurement in more complex solutions is typically experimentally more demanding. To simulate crowded solutions, we used polyethylene glycol PEG 8000, which was used in earlier studies to simulate the effect of molecular crowding[36,47].

The results shed light into the behavior of DNA hybridization rates in free solution at low ionic salt concentrations, see Fig. 6 and SI-13: Small concentrations of PEG < 5% (v/w) facilitated binding and yielded for stronger affinities due to decreased off-rates, possibly due to excluded volume effects. But increasing PEG concentrations from 5% to 10% (v/w) led to increasing off-rates, resulting in reduced affinities. The increased off-rate at higher PEG concentrations may be explained by a destabilizing effect of the surrounding PEG molecules on the hybridized DNA. The on-rates showed weak if no dependence on PEG concnentration.

Our findings highlight that at low ionic salt concentrations, crowding agents affect the DNA hybridization rates not only by excluding volume effects but also by destabilization of the hybridized complex. This result extends earlier studies with FRET measurements which found that kinetic relaxation time constants of DNA hybridization are weakly if not dependent on crowding agent concentrations for higher ionic salt concentrations for 1xPBS[36] and 1xPBS with 1mM Mg^{2+}.[48]

Conclusion

We demonstrated here that the combination of Microscale Thermophoresis with the temperature jump technique provides a novel method to determine kinetic rates together with binding affinities in a single experiment. By a straightforward hardware modification of a conventional MST setup – increasing the thermal dissipation by placement of the sample-containing capillary on a silicon plate and immersion with oil – kinetic relaxation could be extracted from the fluorescence traces. We systematically studied the dependency on salt concentration, strand length and temperature of on- and off- DNA hybridization rates. We found an exponential dependence of the off-rate on strand length, salt and temperature. We further found weak if no dependence at all of the on-rate on temperature and strand length and a linear dependence on salt concentration. The results shed light into the hybridization mechanism of DNA and summarized the determinants of DNA binding. The method allows for measurements of wide salt concentrations and in crowded solutions with minor loss of accuracy, it needs very low sample quantities and it is a very easy-to-use and robust setup. While requiring the probed binding reaction to have a sufficient enthalpic contribution, no artifact-inducing processes, like molecule attachment to surface, are necessary. We believe that KMST could be of great interest for a broad audience - including the numerous labs who have a MST device - and could open new possibilities for researchers in biological and medical sciences.

Acknowledgements

J.A.C.S thanks Ekaterina Khrameshina for assistance with the experiments. Funded by the Deutsche Forschungsgemeinschaft (DFG, German Research Foundation) – Project-ID 364653263 – TRR 235 P11 and the Simons Collaboration on the Origins of Life (Grant #327125FY19).

Keywords: Microscale Thermophoresis • Binding kinetics • DNA hybridization • Kinetic rates • DNA thermodynamics

[1] M. Jerabek-Willemsen, T. André, R. Wanner, H. Marie, S. Duhr, P. Baaske, D. Breitsprecher, *J. Mol. Struct.* **2014**, *1077*, 101–113.

[2] D. J. O'Shannessy, M. Brigham-Burke, K. Karl Soneson, P. Hensley, I. Brooks, *Anal. Biochem.* **1993**, DOI 10.1006/abio.1993.1355.

[3] H. Gohlke, G. Klebe, *Angew. Chemie - Int. Ed.* **2002**, *41*, 2644–2676.

[4] M. M. R. Arkin, J. A. Wells, *Nat. Rev. Drug Discov.* **2004**, *3*, 301–317.

[5] M. M. Morelock, C. A. Pargellis, E. T. Graham, D. Lamarre, G. Jung, *J. Med. Chem.* **1995**, 1751–1761.

[6] E. Helmerhorst, D. J. Chandler, M. Nussio, C. D. Mamotte, *Clin. Biochem. Rev.* **2012**, *33*, 161–173.

[7] S. Xu, J. Zhan, B. Man, S. Jiang, W. Yue, S. Gao, C. Guo, H. Liu, Z. Li, J. Wang, Y. Zhou, *Nat. Commun.* **2017**, 1–14.

[8] T. E. Ouldridge, F. Romano, J. P. K. Doye, S. Petr, A. A. Louis, *Nucleic Acids Researc* **2013**, *41*, 8886–8895.

[9] R. L. Rich, D. G. Myszka, *J. Mol. Recognit.* **2008**, *2008*, 355–400.

[10] Y. Abdiche, D. Malashock, A. Pinkerton, J. Pons, *Anal. Biochem.* **2008**, *377*, 209–217.

[11] J. Regan, C. A. Pargellis, P. F. Cirillo, T. Gilmore, E. R. Hickey, G. W. Peet, A. Proto, N. Moss, *Bioorg. Med. Chem. Lett.* **2003**, *13*, 3101–3104.

[12] J. Knezevic, A. Langer, P. A. Hampel, W. Kaiser, R. Strasser, U. Rant, *J. Am. Chem. Soc.* **2012**, *134*, 15225–15228.

[13] N. R. Mohammad, N. H. C. Marzuki, R. A. Wahab, *Biotechnol. Biotechnol. Equip.* **2015**, *29*, 205–220.

[14] M. M. Baksh, A. K. Kussrow, M. Mileni, M. G. Finn, D. J. Bornhop, *Nat. Biotechnol.* **2011**, *29*, 357–360.

[15] P. R. Edwards, R. J. Leatherbarrow, *Anal. Biochem.* **1995**.

[16] K. Sigmundsson, G. Másson, R. Rice, N. Beauchemin, B. Öbrink, *Biochemistry* **2002**, *41*, 8263–8276.

[17] W. Bujalowski, M. Jezewska, in *Spectrosc. Methods Anal Methods Protoc. Mol. Biol.*, **2012**.

[18] K. Bielec, K. Sozanski, M. Seynen, Z. Dziekan, *Phys.Chem.Chem.Phys* **2019**, *21*, 10798–10807.

[19] Y. Li, P. C. Bevilacqua, D. Mathews, D. H. Turner, *Biochemistry* **1995**, *34*, 14394–14399.

[20] P. Schwille, J. Bieschke, F. Oehlenschläger, *Biophys. Chem.* **1997**, *66*, 211–228.

[21] M. Jerabek-willemsen, C. J. Wienken, D. Braun, P. Baaske, S. Duhr, *Assay Drug Dev. Technol.* **2011**, 342–353.

[22] S. Duhr, D. Braun, *Proc. Natl. Acad. Sci. U. S. A.* **2006**, *103*, 19678–19682.

[23] P. Baaske, C. J. Wienken, P. Reineck, S. Duhr, D. Braun, *Angew. Chemie - Int. Ed.* **2010**, *49*, 2238–2241.

[24] C. J. Wienken, P. Baaske, U. Rothbauer, D. Braun, S. Duhr, *Nat. Commun.* **2010**, DOI 10.1038/ncomms1093.

[25] C. J. Wienken, P. Baaske, S. Duhr, D. Braun, *Nucleic Acids Res.* **2011**, *39*, DOI 10.1093/nar/gkr035.

[26] S. A. I. Seidel, M. Jerabek-Willemsen, D. Braun, S. Duhr, *Methods* **2013**, *59*, 301–315.

[27] S. A. I. Seidel, C. J. Wienken, M. Jerabek-Willemsen, S. Duhr, D. Braun, P. Baaske, *Angew. Chem. Int. Ed.* **2012**, 10656–10659.

[28] E. L. Elson, *Biophys. J.* **2011**, *101*, 2855–2870.

[29] K. M. Parkhurst, L. J. Parkhurst, *Biochemistry* **1995**, *34*, 285–292.

[30] R. L. Rich, L. R. Hoth, K. F. Geoghegan, T. A. Brown, P. K. Lemotte, S. P. Simons, P. Hensley, D. G. Myszka, *Proc. Natl. Acad. Sci. U. S. A.* **2002**, *99*, 8562–8567.

[31] D. G. Myszka, R. L. Rich, *Pharm. Sci. Technol. Today* **2000**, *3*, 310–317.

[32] D. Pörschke, M. Eigen, *J. Mol. Biol.* **1971**, *62*, 361–381.

[33] A. Ianeselli, C. B. Mast, D. Braun, *Angew. Chemie - Int. Ed.* **2019**, *58*, 13155–13160.

[34] K. Tawa, W. Knoll, *Nucleic Acids Res.* **2004**, *32*, 2372–2377.

[35] N. F. Dupuis, E. D. Holmstrom, D. J. Nesbitt, *Biophys. J.* **2013**, *105*, 756–766.

[36] I. Schoen, H. Krammer, D. Braun, *Proc. Natl. Acad. Sci. U. S. A.* **2009**, *106*, 21649–21654.

[37] Y. Okahata, M. Kawase, H. Furusawa, Y. Ebara, *Anal. Chem.* **1998**, *70*, 1288–1291.

[38] W. H. Braunlin, V. A. Bloomfield, *Biochemistry* **1991**, *30*, 754–758.

[39] L. E. Morrison, L. M. Stols, *Biochemistry* **1993**, *32*, 3095–3104.

[40] D. Pörschke, *Biophys. Chem.* **1974**, *1*, 381–386.

[41] K. A. van der Meulen, S. E. Butcher, *Nucleic Acids Res.*

2012, *40*, 2140–2151.

[42] E. D. Holmstrom, D. J. Nesbitt, *Annu. Rev. Phys. Chem.* **2016**, *67*, 441–465.

[43] M. S. Searle, D. H. Williams, *Nucleic Acids Res.* **1993**, *21*, 2051–2056.

[44] C. Chen, W. Wang, Z. Wang, F. Wei, X. S. Zhao, *Nucleic Acids Res.* **2007**, *35*, 2875–2884.

[45] G. Bonnet, O. Krichevsky, A. Libchaber, *Proc. Natl. Acad. Sci.* **1998**, *95*, 8602–8606.

[46] P. J. Doyle, A. Savara, S. S. Raiman, *React. Kinet. Mech. Catal.* **2020**, *129*, 551–581.

[47] L. E. Baltierra-Jasso, M. J. Morten, L. Laflör, S. D. Quinn, S. W. Magennis, *J. Am. Chem. Soc.* **2015**, *137*, 16020–16023.

[48] X. Zhang, P. J. J. Huang, M. R. Servos, J. Liu, *Langmuir* **2012**, *28*, 14330–14337.

Entry for the Table of Contents

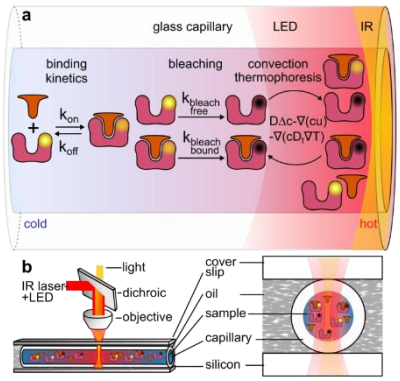

The extension of Microscale Thermophoresis (MST) to perform temperature jumps in less than 250 ms allows for quantification of binding affinities together with the kinetic rates. We measured relaxation kinetics for DNA hybridization with high fidelity at different temperatures, probe configurations and a wide range of buffer conditions. The results shed light into the hybridization mechanism of DNA and confirmed determinants of DNA binding.